

This is a repository copy of *Efficient modelling of thin conducting sheets within the TLM method*.

White Rose Research Online URL for this paper:

<https://eprints.whiterose.ac.uk/90053/>

Version: Accepted Version

Book Section:

Cole, J.A., Dawson, J.F. orcid.org/0000-0003-4537-9977 and Porter, S.J. (1996) Efficient modelling of thin conducting sheets within the TLM method. In: *Computation in Electromagnetics, Third International Conference on* (Conf. Publ. No. 420). IET , pp. 45-50.

<https://doi.org/10.13140/2.1.2628.4320>

Reuse

Items deposited in White Rose Research Online are protected by copyright, with all rights reserved unless indicated otherwise. They may be downloaded and/or printed for private study, or other acts as permitted by national copyright laws. The publisher or other rights holders may allow further reproduction and re-use of the full text version. This is indicated by the licence information on the White Rose Research Online record for the item.

Takedown

If you consider content in White Rose Research Online to be in breach of UK law, please notify us by emailing eprints@whiterose.ac.uk including the URL of the record and the reason for the withdrawal request.

EFFICIENT MODELLING OF THIN CONDUCTING SHEETS WITHIN THE TLM METHOD

J A Cole, J F Dawson and S J Porter

University of York, UK

The paper describes the use of recursive filters to efficiently model the transmission through thin conducting layers in the Transmission Line Matrix (TLM) method of numerical electromagnetic modelling. The technique is applicable where the layer may be many skin-depths thick but thin compared with the mesh size. The technique is validated against an analytical solution, and improved efficiency over other methods is demonstrated. The technique is also applicable to composite layers with complex structures which are not amenable to analytical solution.

INTRODUCTION

The Transmission Line Matrix (TLM) Method, see Johns [1], has been used to model enclosures whose walls are composed of material which is strongly conducting. Typically energy penetration into such enclosures is via apertures and cabling: the walls can be considered to be approximated by a perfect conductor. As such the walls are often incorporated using a sub-grid model boundary between nodes in the TLM mesh. The effects of the walls are modelled using frequency-independent reflection coefficients, typically of value -1 : there is no transmission allowed. This has proved to be successful where the dominant energy penetration mechanism is via apertures or cabling.

In the case where the enclosure walls are composed of thin sheets of a relatively moderately conducting material (for example, materials with conductivities in the range of 1 kS/m to 30 kS/m) and where the energy penetration mechanism is not dominantly through apertures and cabling, using a fixed reflection coefficient and zero transmission coefficient is inadequate. In this case, it is necessary to use boundaries with frequency dependent reflection and transmission coefficients.

Direct incorporation of the walls within the normal TLM mesh is possible, but requires a prohibitively small grid size. Even use of specific sub-grid models of the walls based on standard TLM nodes still results in large computational overheads.

Thin Layer Models

Various methods for circumventing this problem have been tried. Mallik and Loller [2] present a method using a parallel combination of resistors to represent the frequency dependent reflection and transmission properties of thin sheets of conducting materials. This becomes computationally inefficient when many layers of resistance are required to model the composite structure.

Since the lateral propagation in such materials is negligible, the efficiency of the computation can be increased if only propagation through the layer is considered. Johns et al [3]

have proposed such a method using lossy, loaded transmission lines. It is however much more efficient to implement the propagation and reflection using discrete time recursive filters.

Fuchs [4] has succeeded in demonstrating a full analytical, time-domain solution to the transmission through thin conducting layers. His solution is expressed as an infinite sum of decaying exponential terms which can be truncated to produce a solution of similar efficiency to that presented here. It is likely that this solution can also be converted to the series form of convolution used here.

Other thin layer models have been derived for the Finite Difference Time-Domain method. A vast majority of this work is concerned with perfect conductors, for example Kunz et al [5], or infinitely thin sheets, Wu and Han [6]. Other methods such as those described by Maloney [7, 8], and Luebbers [9] primarily consider the modelling of thin conducting sheets of relatively low conductivity. They do not take into account the decay of fields passing into a conductor which is many skin-depths thick.

New thin layer model

The implementation described here is designed in the frequency domain using discrete time recursive digital filters. It is more efficient than the earlier TLM methods, except that of Fuchs, and applicable to composite materials with complex internal structures that cannot be solved by analytical means. The filter algorithm can be determined from measured, frequency-domain data.

Screening ratio and shielding effectiveness

The screening ratio of a closed shell of any material is defined as the ratio of the electric or magnetic field measured inside the shell, \mathbf{E}_2 or \mathbf{B}_2 , and the field measured at the same point, under the same conditions, but in the absence of the shell, \mathbf{E}_1 or \mathbf{B}_1 . The electric and magnetic screening ratios are then

$$Q_E = |\mathbf{E}_2|/|\mathbf{E}_1| \quad Q_M = |\mathbf{B}_2|/|\mathbf{B}_1| \quad (1)$$

A measure of the ability of an enclosure to exclude external fields can then be defined as the shielding effectiveness. The electric and magnetic shielding effectiveness' are then the reciprocal of these in dB's.

IMPLEMENTATION

Analytical transmission equation

It is convenient to work in terms of transmission rather than SE when determining a filter design to mimic the propagation through the material. The transmission through a thin

conducting layer is

$$S_{21} = \frac{(1 - \rho^2)e^{-\gamma t}}{1 - (\rho e^{-\gamma t})^2} \quad (2)$$

where

$$\gamma(\omega) = \sqrt{(j\omega\epsilon + \sigma)j\omega\mu} \quad (3)$$

is the material propagation constant,

$$\rho(\omega) = \frac{Z_m(\omega) - Z_0}{Z_m(\omega) + Z_0} \quad (4)$$

is the reflection coefficient at the free-space/material interface,

$$Z_m = \sqrt{\frac{j\omega\mu}{j\omega\epsilon + \sigma}} \quad (5)$$

is the characteristic impedance of the material, Z_0 is the characteristic impedance of free-space, t is the thickness of the layer, and ω is the angular frequency. The material is defined by its conductivity, σ , permittivity, ϵ , and permeability, μ .

Transmission Filter Design

Amplitude of transmission. At low frequencies, where the skin depth is much greater than the material thickness and where the sheet resistance (R_s) is much less than Z_0 ($R_s \ll Z_0$), the transmission (S_{21}) through the layer can be determined using the infinitesimally thick layer approximation

$$S_{21} = 1 + \rho_t = 1 + \frac{R_s - Z_0}{R_s + Z_0} \quad (6)$$

where ρ_t is the reflection coefficient determined by the resistance per square (sheet resistance) and R_s is the resistance per square (strictly, the parallel combination of the resistance per square and Z_0)

$$R_s = \frac{1}{\sigma t} \quad (7)$$

At high frequencies the attenuation term, $e^{-\gamma t}$, dominates the transmission. Taking these two effects S_{21} can be approximated by

$$S_{21} = \left[1 + \frac{R_s - Z_0}{R_s + Z_0} \right] e^{-\gamma t} \quad (8)$$

This is not a good approximation because the effect of multiple reflections and change of interface reflection coefficient with frequency have a significant effect. The effect is to delay the onset of decrease in transmission due to the loss term. However, the general shape serves as a good basis for an initial filter design to mimic the S_{21} parameter and is more tractable than the full analytic expression for S_{21} .

The initial reflection loss can be modelled as the low frequency gain of a filter whilst the attenuation curve can be approximated by an all-pole filter. In decibels, the attenuation term is

$$A(\omega) = 20 \log |e^{-\gamma t}| \quad (9)$$

Rewriting this, and applying the good conductor approximation, $\gamma = \sqrt{j\sigma\mu\omega}$, we get

$$A(\omega) = 20 \log_{10}(e)t\sqrt{\sigma\mu\omega/2} \quad (10)$$

which, expressed as a function of frequency becomes

$$A(f) = 20 \log_{10}(e)t\sqrt{\sigma\mu\pi f} \quad (11)$$

Putting $x = \log_{10} f$ and hence $f = e^{ax}$, where $a = \ln 10$, then differentiating Eq. 11 with respect to x (log-frequency) we get

$$\frac{dA(x)}{dx} = 20 \log_{10}(e)\frac{at}{2}\sqrt{\sigma\mu\pi}e^{ax/2} \quad (12)$$

in dB/decade, so that the gradient of the attenuation increases exponentially with frequency. All-pole filters tend to a linear increase in attenuation with frequency ($20N$ dB/decade) where N is the number of poles. The number of poles required to simulate this response up to a given frequency is therefore

$$N = \log_{10}(e)\frac{at}{2}\sqrt{\sigma\mu\pi}e^{ax/2} \quad (13)$$

or, expressing N directly as a function of frequency, noting $\ln(10) \log_{10}(e) = 1$,

$$N = 0.5t\sqrt{\sigma\mu\pi f} \quad (14)$$

In practice the number of poles is greater than required by Eq. (14). In order to allow for this in subsequent calculations an empirical factor k_f is added to give the optimum number of poles

$$N_{opt} = 0.5t\sqrt{\sigma\mu\pi f k_f} \quad (15)$$

A value of 2 for k_f has been found to be adequate, which requires 38 poles to simulate the shielding effectiveness of 5 mm, 30 kS/m material up to 1 GHz.

In order to determine the pole placement, Eq. (14) can be rearranged to give the angular frequency of the n th pole. In terms of angular frequency, $\omega(n)$, the position of the n 'th pole is

$$\omega(n) = - \left[\frac{8N^2 k_p}{t^2 \mu \sigma} \right] \quad (16)$$

where the empirical factor k_p is used to account for the difference between the approximate SE given by Eq. (8) and the actual shielding effectiveness. A value of $k_p = 1.233$ gives a good correspondence with the actual SE. Thus, the filter is constructed of N_{opt} poles which lie in the complex s -plane at $s = \omega(n)$ (on the real axis).

The s -plane filter realisation represents a continuous time filter. It can be approximated by a discrete time filter using the impulse invariant transform. For frequencies up to $1/20$ of the sampling frequency, the frequency range over which TLM results are usually considered valid, the discrete time filter response corresponds very closely to the continuous time response. For the 5 mm, 30 kS/m material, the SE is more than 500 dB at 1 GHz. A peak error of 10 dB occurs at the upper design limit of the filter (see Fig. 2). This error is due to the continued exponential (in dB) increase in SE whilst the filter tends to a constant increase in attenuation.

Phase considerations. While the amplitude response of the filter described above shows a good correspondence with the analytical solution, the phase error increases linearly with frequency. This corresponds to a time delay in the physical system which is not present in the filter. This is simple to

remedy in the digital case by adding extra time delay in the filter: a fixed time delay corresponds to a linear increase in phase-shift with frequency. The differential time delay is

$$T_d = \frac{d \arg(S_{21}(\omega)/H_z(\omega))}{d\omega} \quad (17)$$

where S_{21} is the analytical solution and $H_z(\omega)$ is the frequency response of the (digital) filter. A time delay which is an integer number of time steps can easily be implemented by using delayed outputs from each digital filter stage. When this scheme is applied, the peak phase error is 6° at the upper design frequency of 1 GHz.

Digital Filters

The filters described so far can be implemented digitally using the impulse invariant transform to produce 2nd order digital filter sections from the s-plane representation. 2nd order sections are used because:

- higher order sections tend to suffer from greater numerical errors;
- a 2nd order section can realise two real poles and two real zeros or a complex conjugate pair of each.

This section shows how a general 2nd order s-plane transfer function is converted to digital form.

2nd order systems. In general a second order system can be described by the Laplace transform as

$$H(s) = \frac{s^2 2\zeta_n \omega_n s + \omega_n^2}{s^2 2\zeta_d \omega_d s + \omega_d^2} \quad (18)$$

where ζ is the damping factor and $\omega_{n/d}$ the natural frequency (numerator/denominator) of the system. Alternatively the function can be described in terms of its poles and zeros

$$H(s) = K_g \frac{(s - z_{s1})(s - z_{s2})}{(s - p_{s1})(s - p_{s2})} \quad (19)$$

where K_g is a gain constant, p_{s1} and p_{s2} are the s-plane poles of the system and z_{s1} and z_{s2} are the s-plane zeros. The poles and zeros are either real or complex conjugate pairs for any system where the time response is real. The frequency response of the system can be easily evaluated by substituting $s = j\omega$ where ω is the angular frequency and evaluating $H(j\omega)$ at the frequency of interest. The time response can be determined using Laplace transforms.

2nd order recursive filter. The continuous function $H(s)$ can be approximated by the discrete time function

$$H(Z) = \frac{b_0 + Z^{-1}b_1 + Z^{-2}b_2}{1 - Z^{-1}a_1 - Z^{-2}a_2} \quad (20)$$

where Z^{-1} represents a unit delay. This can also be written as

$$H(Z) = \frac{b_0 Z^2 + Z^1 b_1 + b_2}{Z^2 - Z^1 a_1 - a_2} \quad (21)$$

In terms of the Z-plane poles and zeros

$$H(Z) = b_0 \frac{(Z - z_{z1})(Z - z_{z2})}{(Z - p_{z1})(Z - p_{z2})} \quad (22)$$

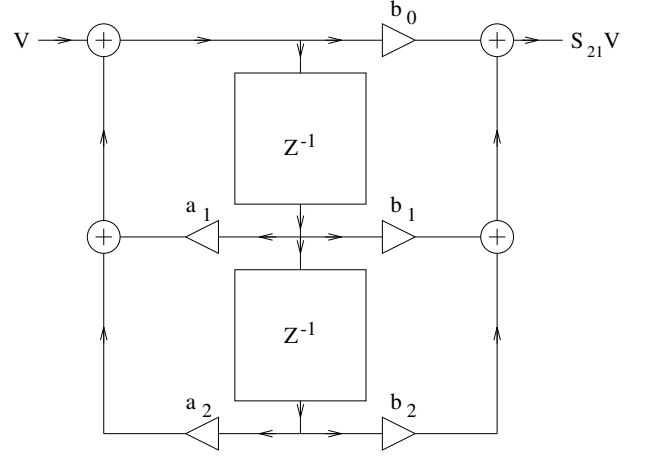


Figure 1: Second order digital filter section

so that

$$a_1 = p_{z1} + p_{z2} \quad a_2 = -p_{z1}p_{z2} \quad (23)$$

and

$$\frac{b_1}{b_0} = -(z_{z1} + z_{z2}) \quad \frac{b_2}{b_0} = z_{z1}z_{z2} \quad (24)$$

The discrete time function of Eqs. (20)-(22) can be implemented using the structure shown in Fig. 1 below. The Z^{-1} block represents a delay of one time step, the triangles represent coefficient multipliers, and the circles represent summation. The input to the filter is shown as V and the output is $S_{21}V$.

The impulse invariant transform. The a and b coefficients can be determined using the impulse invariant transform from $H(s)$ so that

$$a_1 = e^{p_{s1}T} + e^{p_{s2}T} \quad a_2 = -e^{p_{s1}T}e^{p_{s2}T} \quad (25)$$

$$\frac{b_1}{b_0} = -(e^{z_{s1}T} + e^{z_{s2}T}) \quad \frac{b_2}{b_0} = e^{z_{s1}T}e^{z_{s2}T} \quad (26)$$

where T is the sample period for the filter, which can be made equal to the TLM time-step. The overall gain is determined by b_0 .

Reflection Filter Design

The reflection coefficient can be approximated in a similar manner by a filter. Here the design requires both poles and zeros. Space does not permit a full description in this paper.

VALIDATION

The plane wave shielding effectiveness of an infinite sheet of material is shown in Figure 2. The close correspondence of the ideal filter and analytical result can be seen. The real filter in single precision (32 bit floating point) arithmetic has a dynamic range of about 130 dB before numerical errors prevent further increase in SE. This represents an extreme example: for thinner layers or lower conductivities the 130 dB dynamic range is not a limiting factor.

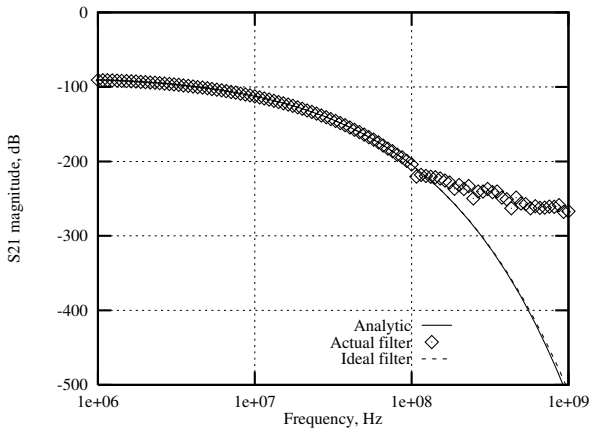


Figure 2: Plane wave transmission for a sheet 5 mm thick with $\sigma = 30$ kS/m.

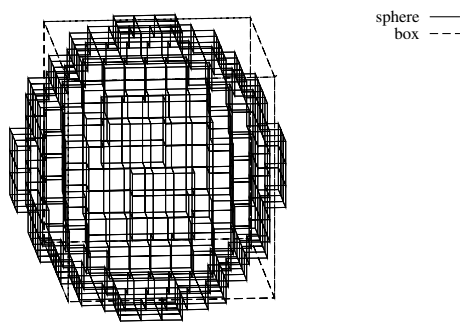


Figure 3: Geometry for cubic box and discretised sphere of same volume.

The shielding effectiveness of spherical cavities are compared with the exact, analytical, sub-resonant calculations of Field [10]. Results are also presented for the shielding effectiveness of a cubic cavity and compared with the calculations of Field for spherical cavities of similar volume. In general agreement is within the 10 dB deviation claimed by Field for objects of the same volume, but there are some anomalies for materials with conductivities in the 1–30 kS/m range. Figure 3 shows the discretisation of the sphere along with a cubic enclosure of the same volume.

Figures 4 to 9 compare the computed (new TLM model) screening ratios for various spherical enclosures with the analytical solution of Fields [10], and the results obtained with the simple fixed transmission boundaries. It can be seen that the new TLM model corresponds closely with the results of Field whilst the fixed transmission boundary diverges at a frequency where the material skin-depth becomes significant. The resonant behaviour of the enclosure is not predicted by Field, so the enclosure parameters were chosen to avoid resonant behaviour over most of the frequency range. Figures 10, 11, and 12 show the computed screening ratios for a cubic box and sphere of the same volume. In general agreement is within the 10 dB deviation predicted by Field, but there are some anomalies for materials with conductivities in the 1–30 kS/m range.

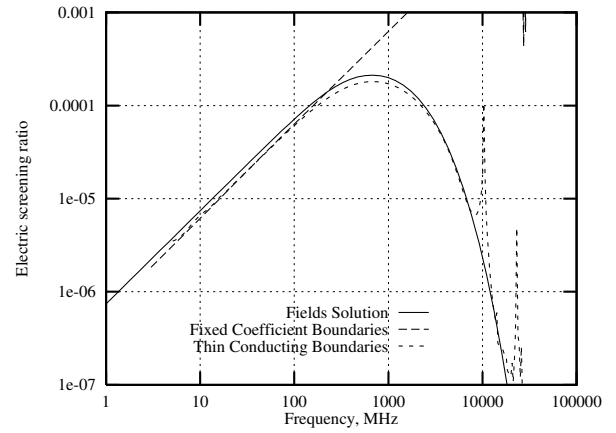


Figure 4: E field screening ratio for sphere, $\sigma = 1.5$ kS/m, radius = 1.24 cm, thickness = 1.5 mm.

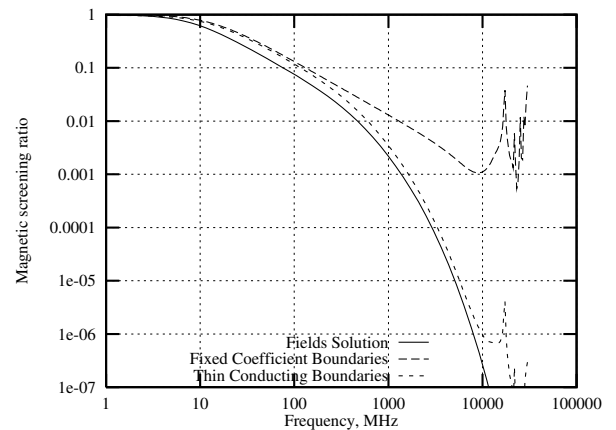


Figure 5: H field screening ratio for sphere, $\sigma = 1.5$ kS/m, radius = 1.24 cm, thickness = 1.5 mm.

DISCUSSION

In general the validation indicates that the method is both an efficient and reliable procedure for the incorporation of materials of reasonably high conductivity that cannot be approximated by frequency-independent, perfectly conducting models.

Efficiency

For 5 mm thick material with a conductivity of 30 kS/m, Eq. (15) indicates that the magnitude of the plane wave shielding up to 1 GHz could be simulated using a filter of order 38 if the additional time delay and reflection are not required. If they are, then extra filter stages are required and the number of poles will be $38+30+12=80$.

The number of poles required will vary with the material thickness, conductivity, and frequency range required. Each filter pole (and each filter zero) requires one storage location, 1.5 multiply and accumulate and one exchange of values (for each pole and zero). Four filters in total would be required for two polarisations in two directions of propagation, so a total of:

- 152 (+120+48=320) storage locations
- 228 (+0+144=372) multiply operations

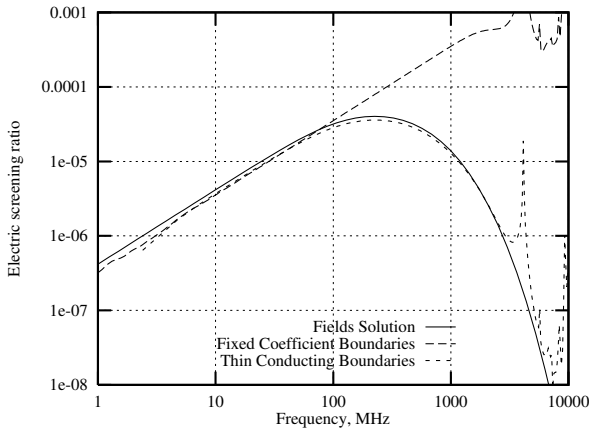


Figure 6: E field screening ratio for sphere, $\sigma = 10$ kS/m, radius = 3.1 cm, thickness = 1 mm.

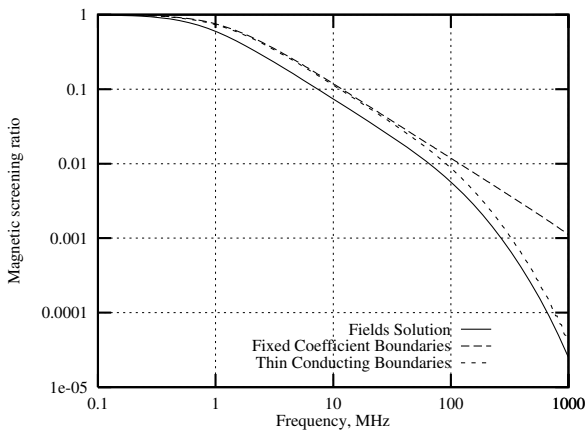


Figure 7: H field screening ratio for sphere, $\sigma = 10$ kS/m, radius = 3.1 cm, thickness = 1 mm.

- 228 (+0+144=372) addition operations
- 152 (+120+48=320) exchanges

would be required per mesh element for this case. The numbers in brackets indicate the number of poles to be added if the additional time delay and reflection are to be modelled. Note that delay requires no multiply and addition operations, reflection requires twice as many.

Comparing with the method of Johns et al [3], the use of 5 mm material with conductivity equal to 30 kS/m corresponds to 54 skin depths at 1 GHz. Four sections of lossy line per skin depth are required by this method. Each section of lossy line requires (at least) 2 storage locations and 4 multiply and accumulate instructions. With one path for each polarisation, this method would require:

- 864 storage locations
- 1728 multiply operations
- 1728 addition operations

The number of exchanges is not evident but is likely to be of the order of 864. This takes the most optimistic solution time for this method, assuming a linear increase in computation with number of sections. In fact Trenkic [11] states

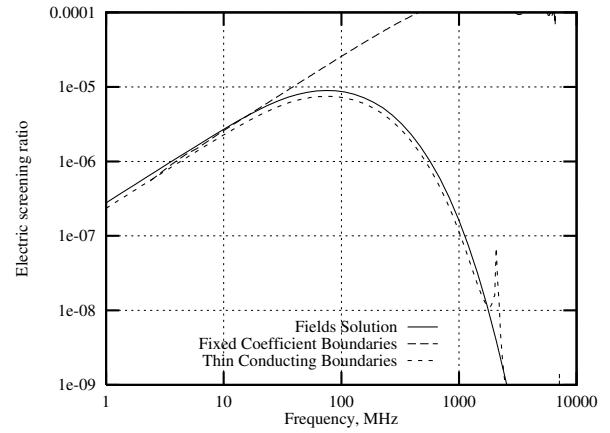


Figure 8: E field screening ratio for sphere, $\sigma = 30$ kS/m, radius = 6.2 cm, thickness = 1 mm.

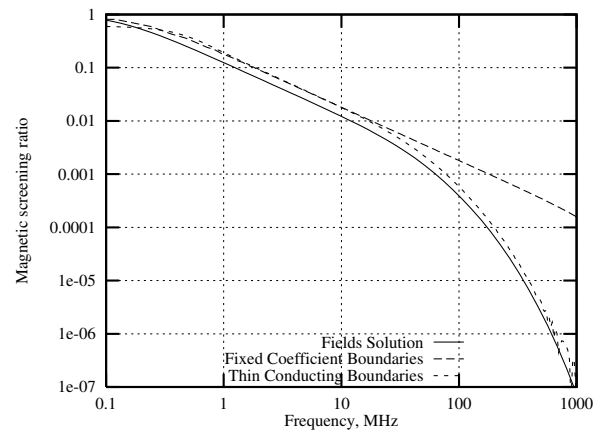


Figure 9: H field screening ratio for sphere, $\sigma = 30$ kS/m, radius = 6.2 cm, thickness = 1 mm.

that the original method used required a number of operations proportional to the square of the number of sections. Trenkic improved this to a linear dependence. Comparing our method with the improved method of Trenkic [11], where the same number of sections are required as Johns et al, this results in:

- 864 storage locations
- 1296 multiply or divide operations
- 864 Additions or subtractions

The method proposed in this paper offers an improvement in computation of about 3.5:1 and storage of about 2.7:1 over the method of Trenkic.

Other Applications

The method described in this paper uses filter design techniques to approximate the transmission through and reflection from a thin conduction layer. A solution was achieved by an empirical approximation to an analytical solution. One significant feature of this technique is that filter design techniques can be applied to approximate transmission/reflection boundaries from measured data for materials which may not be amenable to analytical solution. An additional feature of this implementation is that it allows for the modelling of

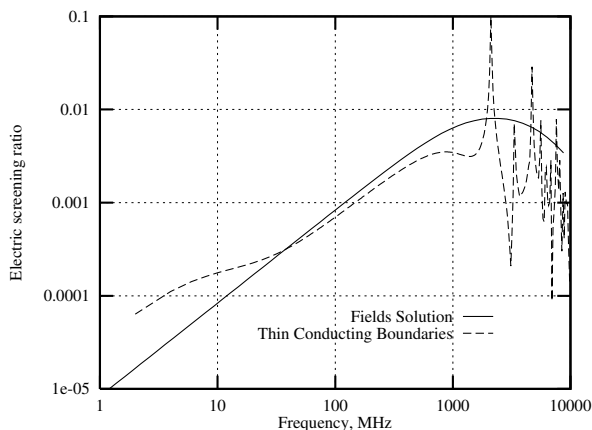


Figure 10: E field screening ratio for box, $\sigma = 1$ kS/m, side = 10 cm.

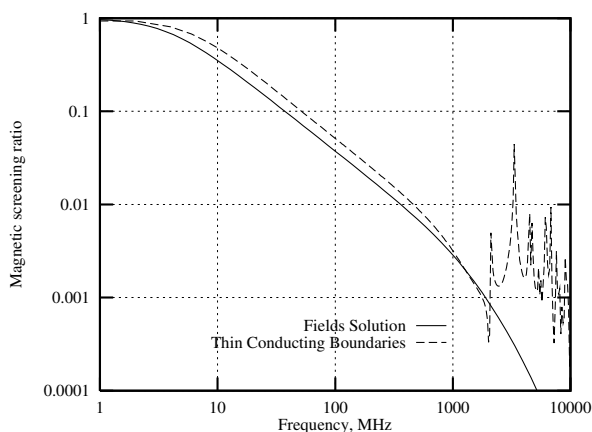


Figure 11: H field screening ratio for box, $\sigma = 1$ kS/m, side = 10 cm.

boundaries with resonant reflection/transmission characteristics.

ACKNOWLEDGEMENTS

The Authors would like to thank British Aerospace, Lucas Applied Technology Ltd., EPSRC, Courtaulds Aerospace Ltd., D.G. Teer Coatings who have supported this work.

REFERENCES

- [1] P.B. Johns and R.L. Beurle. Numerical solution of 2-dimensional scattering problems using a transmission-line matrix. *Proc. Inst. Elec. Eng.*, 118(9):1203–1208, 1971.
- [2] A. Mallik and C. P. Loller. The modelling of EM leakage into advanced composite enclosures using the TLM technique. *Int. J. Num. Mod., Elec. Net., Dev. Flds*, 2(4):241–248, 1989.
- [3] D.P. Johns, J. Wlodarczyk, and A. Mallik. New TLM models for thin structures. In *IEE Proc. Int. Conf. Comp. Electromag.*, pages 335–338, 1991.

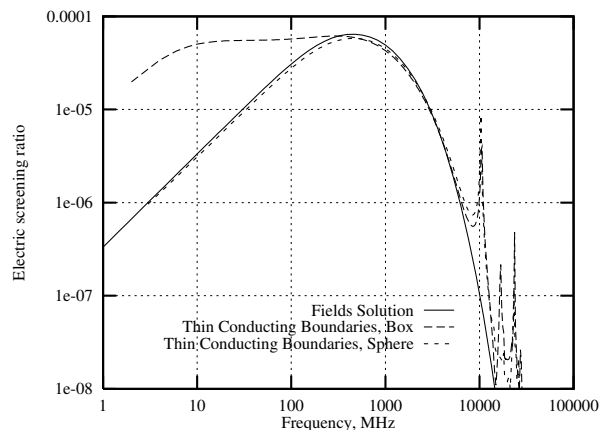


Figure 12: E field screening ratios for box and sphere of equal volume, $\sigma = 5$ kS/m, box side = 2 cm.

- [4] Ch. Fuchs and A. J. Schwab. Efficient computation of 3D shielding enclosures in time domain with TLM. In *COST 243 Workshop, Numerical Methods and their Applications*, Hamburg, June 1995.
- [5] K.S. Kunz, D.J. Steich, and R.J. Luebbers. Low frequency shielding effects of a conducting shell with an aperture: Response of an internal wire. *IEEE Trans. Ant. Prop.*, pages 370–373, 1992.
- [6] Lin-Kun Wu and Liang-Tung Han. Implementation and application of resistive sheet boundary condition in the finite difference time domain method. *IEEE Trans. Ant. Prop.*, 40(6):628–632, 1992.
- [7] J.G. Maloney and G.S. Smith. A comparison of methods for modelling electrically thin dielectric and conducting sheets in the finite-difference time-domain (FDTD) method. *IEEE Trans. Ant. Prop.*, 41(5):690–694, 1993.
- [8] J.G. Maloney and G.S. Smith. The efficient modeling of thin material sheets in the finite-difference time-domain (FDTD) method. *IEEE Trans. Ant. Prop.*, 40(3):323–330, 1992.
- [9] R.J. Luebbers and K. Kunz. FDTD modeling of thin impedance sheets. *IEEE Trans. Ant. Prop.*, 40(3):349–351, 1992.
- [10] J.C.G. Field. An introduction to electromagnetic screening theory. In *IEE Colloq. on Screening and Shielding*, volume Digest no. 83/88, 1983.
- [11] V. Trenkic, C. Christopoulos, and T. M. Benson. Numerical simulation of polymers and other materials for electronic shielding applications. In *Poly. Tech. for Elec. (POLYMAT '94)*, pages 384–7, London, September 1994.